Journal of Hazardous Materials 170 (2009) 560–569

Contents lists available at ScienceDirect

Journal of Hazardous Materials

journal homepage: www.elsevier.com/locate/jhazmat

Review

Strategies of making TiO_2 and ZnO visible light active

Shama Rehman*, Ruh Ullah, A.M. Butt, N.D. Gohar

Nanotechnology Research Group, School of Electrical Engineering and Computer Science (SEECS), National University of Sciences and Technology (NUST), Sector H-12, Islamabad, Punjab 44000, Pakistan

ARTICLE INFO

Article history:
Received 26 January 2009
Received in revised form 13 May 2009
Accepted 14 May 2009
Available online 21 May 2009

Keywords:
Visible light sensitization
Band gap modification
Oxygen vacancies
Impurity states

ABSTRACT

In modern purification techniques employing semiconductor mediated photooxidation of toxic substances, zinc oxide (ZnO) and titanium dioxide (TiO_2) are the most widely used metal oxides due to their unique blend of properties. However, the band edges of these semiconductors lie in the UV region which makes them inactive under visible light irradiation. Researchers have been interested in the modification of electronic and optical properties of these metal oxides for their efficient use in water and air purification under visible light irradiation. Visible light activity has been induced in TiO_2 and ZnO by surface modification via organic materials/semiconductor coupling and band gap modification by doping with metals and nonmetals, co-doping with nonmetals, creation of oxygen vacancies and oxygen sub-stoichiometry. This paper encompasses the progress and developments made so far through these techniques in the visible light photocatalysis with TiO_2 and ZnO. Recently, nitrogen doping in titania has been extensively carried out and therefore somewhat detailed discussion in this respect has been presented. Visible light activation of titania clusters encapsulated in zeolite-Y by nitrogen doping and incorporation of dye or organic sensitizers inside the zeolite framework, has also been highlighted in this review.

Contents

1. Introduction

Apart from the obvious effects of fossil fuels in environmental depletion, the escalating costs of crude oil in international markets have created urgency for utilization of alternative sources of energy. Worldwide efforts are underway to make use of sunlight for energy

* Corresponding author. Tel.: +92 3335199478.
E-mail addresses: shama.rehman@niit.edu.pk, shama_r4@yahoo.com (S. Rehman).

0304-3894/$ – see front matter © 2009 Elsevier B.V. All rights reserved.
doi:10.1016/j.jhazmat.2009.05.064

production, environmental protection and water purification. Sunlight consists of about 5–7% UV light, 46% visible light and 47% infrared radiation [1]. Photocatalytic oxidation of various harmful organic dyes and inorganic pollutants in industrial wastewater has been carried over TiO_2 and ZnO semiconductor oxides under UV light irradiation. Research is now focused on to achieve high photocatalytic efficiency with these materials especially with visible light.

The pre-requisite for an efficient photocatalyst is that the redox potential for the evolution of hydrogen and oxygen from water and for the formation of active species like hydroxyl radicals ($OH^{\bullet}$), hydrogen peroxide (H_2O_2) and super oxide ($O_2^{\bullet -}$) should lie within the band gap of a semiconductor photocatalyst [2]. Since photocatalytic reaction proceeds in air saturated and water rich environment, the employed catalyst should remain stable under these conditions. Narrow band gap semiconductors such as Fe_2O_3 (E_g = 2.3 eV), GaP (E_g = 2.23 eV) and GaAs (E_g = 1.4 eV) which can absorb visible light are unstable in aqueous suspensions and therefore are not suitable for photocatalytic applications [1]. TiO_2 which has a band gap of 3.2 eV [3] is superior to other semiconductor oxides due to its high chemical stability, low cost and nontoxic nature [4]. ZnO which has a similar band gap of about 3.2 eV [5] is sometimes preferred over TiO_2 for degradation of organic pollutants due to its high quantum efficiency [6], however, it photocorrodes in acidic aqueous suspensions [7,8]. Under UV light irradiation, both TiO_2 and ZnO are highly efficient photocatalysts since their photogenerated electrons and holes are highly oxidizing and reducing agents respectively [4].

Unfortunately, TiO_2 and ZnO which are benchmarks of UV photocatalysis are inactive under visible light due to their wide band gaps [3,5]. Hence inherent in them is the inability to make use of the vast potential of solar photocatalysis. Various techniques have been employed to make them absorb photons of lower energy as well. These techniques include surface modification via organic materials [9–20] and semiconductor coupling [21–25], band gap modification by creating oxygen vacancies and oxygen sub-stoichiometry [26–28], by nonmetals including co-doping of nonmetals [29–75] and metals doping [76–102]. The developments made so far through these efforts have been elucidated in this review study. In addition, visible light sensitization of titania by spatial structuring [103] and activation of TiO_2 clusters incorporated in the micropores of zeolite under visible light irradiation by chemical means is also described [103–106].

2. Surface modification via organic materials and semiconductor coupling

2.1. Dye sensitization

Dye sensitization has been demonstrated as a useful tool to induce visible light photocatalysis on the surface of wide band gap semiconductors like TiO_2 which are otherwise inactive under visible light [9–14]. Physical adsorption of dyes occurs through the weak Van der Waals interaction between the dye molecule and the surface of semiconductor. Dye sensitization facilitates electron transfer between the dye molecules and the host semiconductor [15].

Various dyes such as 8-hydroxyquinone (HOQ), methylene blue (MB), acid red 44, reactive red dye 198 (RR 198), eosin-Y, merbromine, 2′,7′-dichlorofluorescein, rhodamine B and rhodamine 6G have been used to sensitize TiO_2 particles to visible light [10–14]. The structures of eosin-Y (an azo dye) and MB (a non-azo dye) are shown in Fig. 1. These surface adsorbed dye molecules are excited upon illumination by visible light and inject electrons into the conduction band (CB) of host semiconductor. According to most of the

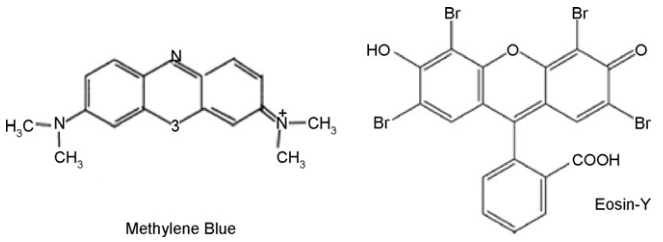

Fig. 1. Structure of eosin-Y and methylene blue.

reports, this injection is favorable due to the more negative potential of the lowest unoccupied molecular orbital (LUMO) of the dye molecules as compared to the conduction band potential of TiO_2 (Fig. 2). However, an exact location of these molecular orbitals of the dyes with respect to the CB of TiO_2 needs to be mentioned to support the proposed mechanism of electron transfer. The electrons injected by dye molecules hop over quickly to the surface of titania where they are scavenged by molecular oxygen to form superoxide radical $O_2^{\bullet -}$ and hydrogen peroxide radical $^{\bullet}OOH$.

$$e^- + O_2 \rightarrow O_2^{\bullet -}$$

$$O_2^{\bullet -} + H^+ \rightarrow {}^{\bullet}OOH$$

These photoactive radicals decolorize and mineralize substrate dyes by destroying their chromophore structure [10,11,15]. For organic pollutants other than dyes, these radicals attack their aromatic rings forming intermediates and mineralizing them to carbon dioxide and water. The extent of pollutant degradation by dye sensitized TiO_2 depends on the nature and adsorption capability of the substrates. The adsorbed dye gets oxidized upon electron injection to the CB of TiO_2 but they are reduced back to their original oxidation state either by accepting electrons from electron donor like aqueous triethanolamine solution (TEOA aq.) or from adsorbed pollutants [10,11,14]. In case of MB, oxidation of the dye follows the reduction process [11].

The quantity of the dye adsorbed on the surface of the photocatalyst is of foremost importance since only this amount contributes to photocatalytic process and not the one in the bulk of the solution. The extent of dye adsorption depends on the initial dye concentration [13], nature of the dye, surface area of photocatalyst and pH of the solution [12,13]. pH of the solution determines the surface charge of the photocatalyst. Adsorption of the dye is minimum at the pH of the solution where the surface of the photocatalyst carries no electric charge (isoelectric point or point of zero charge). The surface of the photocatalyst is positively charged below isoelectric point and carries a negative charge above it. Depending on the nature of dye that needs to be adsorbed on the surface of a photocatalyst, the adsorption can be low or high in acidic and basic media [12]. For instance, adsorption of acid dyes such as eosin and

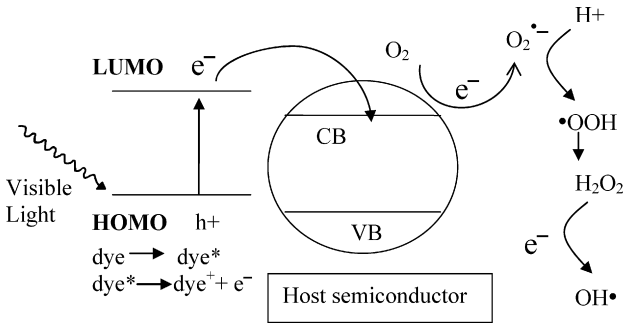

Fig. 2. Visible light activation of a wide band gap semiconductor by dye sensitization.

acid red 44 is favorable at pH below isoelectric point. Higher the surface area of the photocatalyst, higher will be the adsorption sites for the dyes. The visible light activity of reactive red dye 198 sensitized TiO_2 increased upon ultrasonication which deagglomerated titania particles increasing surface active sites for dye or substrates adsorption [13].

Unlike UV photocatalytic process, where an e–h pair is generated in the wide band gap semiconductor, in dye sensitized visible light photocatalysis no hole exists in the valence band of the semiconductor corresponding to injected electrons in the CB and therefore no change in pH of the solution is observed with the course of photocatalytic reaction under visible light irradiation [12]. Owing to the high concentration of pollutant in comparison to the adsorbed dye the self-degradation of the adsorbed dyes is kinetically unfavorable in the presence of pollutants. The dyes themselves are attacked by the active species after the pollutants have been degraded [11,13]. Dye sensitized TiO_2 shows appreciable visible light activity only until the adsorbed dye is itself not degraded. It is therefore not a reusable photocatalyst.

Dye sensitization is a powerful technique to make TiO_2 sensitive to visible light but frequent desorption of dye molecules significantly reduces the potential use of this technique for practical applications. To avoid desorption, eosin-Y dye has been chemically affixed to platinized TiO_2 particles through silane coupling reagent [14]. Although this chemical fixation prevents photobleaching of eosin-Y but silane coupling reagent hinders electron transfer process from excited dye to CB of TiO_2. The visible light activity of chemically fixed dye thereby remains lower than that of physically mixed system of dye and Pt/titania [14].

2.2. Surface-complex assisted sensitization

In surface modification techniques like dye sensitization, desorption of dye molecules can severely affect the visible light activity of the photocatalyst [16]. Surface-complex assisted sensitization has proved to be a much better alternative to dye sensitization in this respect. In this technique a surface complex is formed between organic compounds (other than the dyes) and the host photocatalyst via strong chemical bonds [16–18]. This surface complex is sensitive to visible light and injects electrons into the CB of the host semiconductor as illustrated in Fig. 3. The rest of the mechanism is the same as that of dye sensitization.

Li et al. [17] proposed two different surface complexes to explain the observed visible light activity of anatase titania nanoparticles. The surface complex formed due to the condensation reaction between the hydroxyl group of adsorbed substrate (phenol, 4-chlorophenol (4-CP), 4-hydroxybenzoic) and Ti^{4+}-OH acted as sensitizer to visible light whereas the complex Ti^{4+}-OCR formed due to the reaction between organic moieties formed by autoclaving and Ti^{4+}-OH, trapped these injected electrons [17]. Stepwise removal of the Ti^{4+}-OCR complex by annealing led to a decline in visible light activity. Free hydroxyls on the surface of TiO_2 formed a surface complex with –NCO groups of tolylene diisocyanate (TDI) via a strong –NHCOOTi chemical bond [16,18]. With an increase in TDI content, visible light absorption by the surface complex formed in case of TDI-modified TiO_2 increased accompanied by a faster rate and higher extent of MB degradation [16]. Jiang et al. [18] further improved the visible light activity of TDI-modified TiO_2 by linking one –NCO group of TDI with Ti^{4+}-OH and other with NH_2 group of chrysoidine G (CG) dye. This resulted in the formation of a donor–acceptor type π-conjugated surface complex on the surface of titania which readily absorbed visible light and ultimately injected electrons in the CB of titania. A direct contact between the titania surface and the adsorbed substrate was prevented by the dye layer [18]. The extent of substrate degradation depends on the adsorption capacity of the surface complex formed [18]. Moreover, the surface complex can undergo self-degradation during the photocatalytic reaction and can lower the visible light activity of the photocatalyst.

2.3. Polymer sensitization

Both ZnO and TiO_2 have been surface sensitized with conjugated polymer poly(fluorine-co-thiophene) (PFT) instead of a dye resulting in light absorption up to 500 nm wavelength [19,20]. The conjugated polymer PFT plays the same role as that of a dye in dye sensitization. The reductive potential of PFT is weaker than that of TiO_2 and ZnO and promotes injection of its excited electrons to the conduction band of these semiconductors [19,20]. Polymers are stable sensitizers in water compared to dyes because of their low solubility in water. This is why much higher degradation rate of phenol with TiO_2/PFT is observed than with TiO_2/rhodamine B [19]. When ZnO was sensitized with PFT the substrates, methyl orange and phenol were degraded only to a small extent under visible light illumination [20].

2.4. Semiconductor coupling

TiO_2 has been coupled with narrow band gap semiconductors like Bi_2S_3 [21], CdS [21–23], CdSe [24] and V_2O_5 [25] which are capable of absorbing visible light. The basic principle of this technique is similar to dye sensitization except that instead of an organic dye the sensitizer is a narrow band gap semiconductor. The sensitizer semiconductor absorbs visible light and injects electrons into the CB of titania which remains inactive with visible light. These injected electrons can move to the surface of TiO_2 particles and engage to produce active oxidative species as can be seen in Fig. 4. The presence of Ti^{3+} peak (g = 1.9920) in Electron Spin Resonance (ESR) spectra for coupled semiconductors and its absence for pure titania confirms the photoinjection mechanism of electrons from sensitizer semiconductor to TiO_2 [22,24].

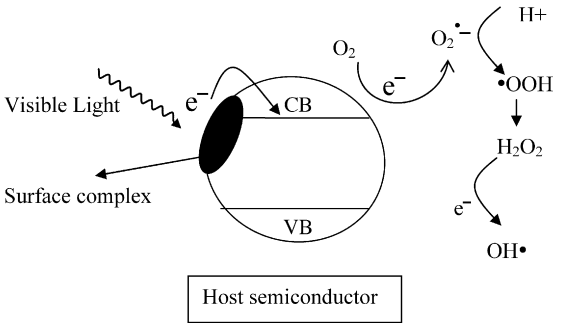

Fig. 3. Visible light activation of a wide band gap semiconductor with surface-complex assisted sensitization.

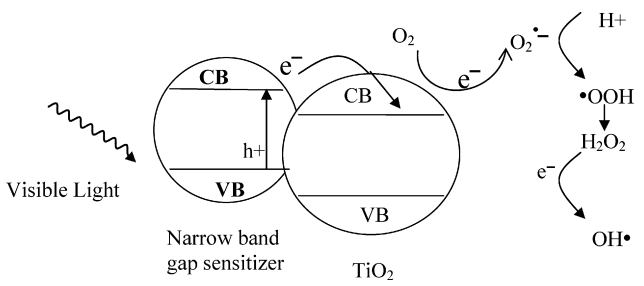

Fig. 4. Visible light activation of TiO_2 by coupling with a narrow band gap semiconductor.

The efficient electron and hole transfer between the sensitizer and TiO_2 depends on the difference between the respective conduction band and valence band potentials of the two semiconductors respectively [21,24]. The conduction and valence band potentials of TiO_2 should be more negative and less positive respectively than that of the sensitizer. Alternatively, the CB of narrow band gap semiconductor should be higher than that of titania and its valence band (VB) need to be lower than that of TiO_2 [10,21,24]. The greater the difference in the band potentials of the two semiconductors, higher is the interfacial charge transfer and vice versa. The conduction band potentials of TiO_2, Bi_2S_3, CdS, and CdSe versus Normal Hydrogen Electrode (NHE) at pH 7 are −0.5 V, −0.76 V, −0.95 V and −1.0 respectively [21,24]. Although the conduction band minima of CdS is much higher than that of Bi_2S_3, the visible light activity of CdS/TiO_2 heterojunction is reported to be much lower than that of Bi_2S_3/TiO_2 junction [21]. This is because Bi_2S_3 absorbs light with wavelengths as high as 800 nm in comparison to CdS which only absorbs light up to 600 nm [21]. This indicates that in addition to the proper location of the band edges of two coupled semiconductors, the extent of visible light absorption of the sensitizer is also crucial for deciding the observed visible light activity of coupled semiconductors. Much higher degradation efficiency of 4-CP was achieved under visible light illumination when CdSe quantum dots coupled to TiO_2 were used as photocatalyst [24]. Owing to quantum confinement effect, the band gap of CdSe quantum dots blue shifts with respect to bulk CdSe (E_g = 1.74 eV) which favors electron injection into the CB of titania [24].

Similar to dye sensitization, the amount of the narrow band gap semiconductor in contact with TiO_2 surface determines the visible light activity of this coupled system. Both visible light absorption and degradation of MB with composite CdS/TiO_2 nanoparticles under visible light irradiation enhanced with an increase in the CdS content [22]. However, with higher concentration of the sensitizer the surface of the host semiconductor can be covered entirely inhibiting surface redox reactions.

By coupling titanium dioxide with a narrow band gap semiconductor, its photoresponse is extended to the visible region and charge carrier separation is achieved [21–25]. In coupled semiconductors, the VB of sensitizer is higher than that of titania which prevents promotion of visible light generated holes in the VB of sensitizer to the VB of titania extending charge carriers lifetime [21–25]. Under UV–vis irradiation both semiconductors are active. This results in an increase in electron population in the CB of TiO_2 in which electrons are injected not only from the sensitizer but also excited from its own VB. TiO_2 can transfer its photogenerated holes to the sensitizer increasing the hole concentration in the VB of sensitizer [21]. This accumulation of charge carriers increases the probability of electron–hole recombination which can significantly reduce the photocatalytic activity of coupled system. Since holes are left behind in the valence band of narrow band gap semiconductors they can photocorrode it if not engaged in redox reactions. Photocorrosion of CdS to Cd has been reported for CdS/TiO_2 system when irradiated with visible light [22]. To prevent photocorrosion of CdS, Ji et al. used sulfite/sulfide which acted as electron donors [23]. High hydrogen production was achieved from seawater over CdS/TiO_2 nanocomposite in the presence of this sacrificial reagent [23].

3. Band gap modification by creation of oxygen vacancies and oxygen sub-stoichiometry

TiO_2 is reported to absorb visible light via artificially created oxygen vacancies in its crystal structure [26,27]. Nakamura et al. generated oxygen vacancies in TiO_2 by plasma treatment through radio-frequency discharge [26]. According to Ihara et al. [27], the oxygen vacancies can be easily created in the grain boundaries of the polycrystalline samples which form a grain boundary defect state in the band gap of titania. Oxygen vacancies facilitate visible light absorption by generating discrete states about 0.75 eV and 1.18 eV below the conduction band of TiO_2 [26]. Oxygen vacancies are active electron traps. Since the oxygen defect states lie close to the CB of titania, the electrons captured by oxygen defects can be promoted to the surface by visible light absorption where they engage in degradation of pollutants [26]. A decline in the reflectance from 380 to 550 nm was noted for oxygen deficient TiO_2 samples [27] while the photoresponse extended to about 600 nm for plasma treated TiO_2 [26].

Justicia et al. [28] observed visible light response with sub-stoichiometric TiO_2 anatase films. The overlap of defect states generated by oxygen sub-stoichiometry with the CB states of TiO_2 reduces its band gap [28].

Alternatively, doping with metals/nonmetals may be done to tailor the electronic and optical properties of ZnO and TiO_2.

4. Band gap modification by nonmetals doping

4.1. Nitrogen doping

Visible light response has been stimulated in both ZnO [29–31] and TiO_2 [32–56] by nitrogen doping. In ZnO nitrogen is proposed to substitute for O sites [29–31]. N acts as an acceptor impurity in ZnO and makes it a p-type material [31]. In titania, nitrogen doping can result in such nitrogen species as substitutional nitrogen N_s or interstitial nitrogen N_i (also mentioned as N_x species), substitutional NO $(NO)_s$, interstitial NO $(NO)_I$ and substitutional NO_2 $(NO_2)_s$ (also referred as NO_x species) [32]. The NO_x species are most likely present on the surface of titania or trapped in the voids of the solids [32–34] but the interstitial or substitutional nitrogen is preferably present in subsurface layers [34]. Nitrogen has also been reported to simultaneously substitute for both O and Ti sites in TiO_2 to form $Ti_{1-y}O_{2-x}N_{x+y}$ (x = 0.36; y = 0.27) instead of $TiO_{2-x}N_x$ [35].

According to Li et al. substitutional N doping generates a new band close to the VB of ZnO with which electrons from the valence band of ZnO makes a two step transition to the conduction band using visible light as depicted in Fig. 5 [29,30]. Density of states calculation made by Asahi et al. [32,36] conclude that substitutional nitrogen species generate states just above the valence band maxima that can mix with O 2p valence states to narrow the band gap of

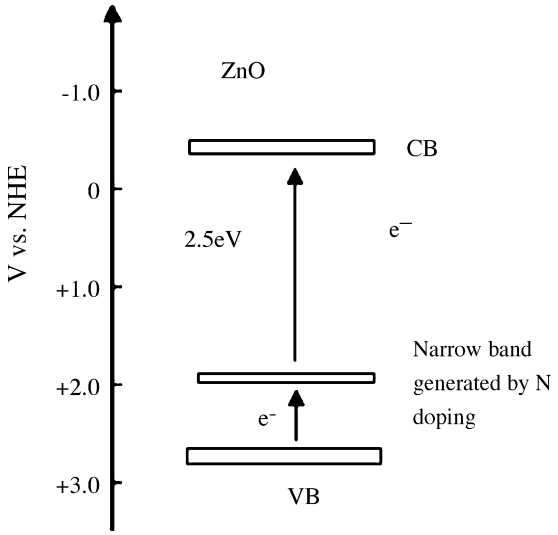

Fig. 5. Visible light absorption by nitrogen doped ZnO.

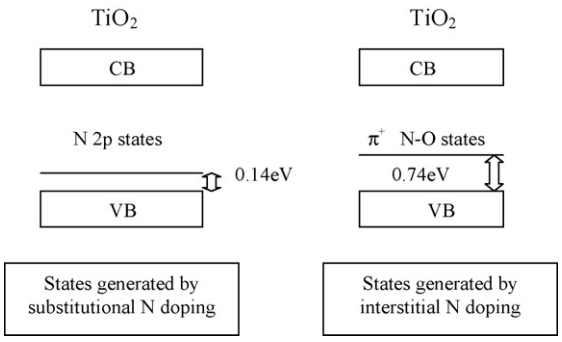

Fig. 6. States generated by substitutional and interstitial N doping in titania according to Refs. [33,34].

TiO_2. Interstitial nitrogen atom couples with a lattice oxygen atom to form a NO unit (different from NO species) to form molecular antibonding states deep in the band gap of TiO_2. Calculations of Valentin et al. [33,34] show that N_s introduce localized nitrogen states about 0.14 eV above the valence band maxima (VBM) and N_i form π-character states about 0.74 eV above the VBM (Fig. 6). These newly generated states are occupied either singly (neutral paramagnetic N_b^*) or doubly (diamagnetic N_b^-).

TiO_2 absorbs visible light when doped with nitrogen. This might not be solely due to substitutional or interstitial nitrogen (N_x). NO_x species can also contribute to visible light absorption since they also generate intragap states like N_s or N_i [32]. Contrary to this Valentin et al. [33,34] claimed that NO or NO_2 trapped in the microvoids of the N doped TiO_2 samples do not modify electronic structure of titania. It should be pointed out that visible light absorption does not ensure high visible light activity. More importantly, it is the location of the impurity states generated in the band gap of TiO_2 by nitrogen doping that determines the visible light activity of these samples. Visible light activity of nitrogen doped samples can be significantly reduced if these newly developed impurity states lay deep in the band gap of titania since they serve as recombination centers [32].

Shen et al. [37] prepared N doped TiO_2 nanoparticulate films by low energy ion implantation method. They found N in the interstitial sites of TiO_2 lattice due to very low energy of implantation. Contrary to the calculations of Asahi et al. [36] these films showed appreciable visible light activity. As much as 50% of MB was degraded by N doped TiO_2 films with highest 3.4% N concentration under visible light irradiation. Peng et al. [38] showed that both substitutional and interstitial N doping in TiO_2 greatly enhanced visible light absorption. Photodegradation of methyl orange and phenol was higher with interstitial N–TiO_2 than with substitutional N–TiO_2 under visible light irradiation. Based on Valentin [33,34] calculations, Peng et al. [38] assumed that the excitation from the highest localized state of interstitial N (0.73 eV above the top of VB) to CB is more favorable in comparison to that from the top of localized state of substitutional N (0.14 eV above the top of VB) under the visible light irradiation. The quantum yield is expected to be the same under both UV and visible light if the band gap narrows with nitrogen doping. Observing a much lower quantum yield of $TiO_{2-x}N_x$ samples under visible than under UV light irradiation, Irie et al. [39] and Sato et al. [40] proposed that substitutional N formed an isolated narrow band just above the valence band edge of TiO_2. UV light excited electrons from both valence band and N 2p isolated band to the conduction band of titania while visible light excited only impurity band electrons to the CB of TiO_2 which resulted in a lower quantum yield [39,40]. Chen et al. [41] carried out X-ray spectroscopic studies on the nitrogen doped rutile TiO_2 bulk samples. They concluded that isolated electronic states were introduced in the band gap of titania above the valence band edge due to nitrogen doping.

Various types of nitrogen species that can be possibly formed in the TiO_2 lattice by N doping are detected through X-ray photoelectron spectroscopy (XPS). Asahi et al. [36] assigned the peaks of N 1s core levels with binding energy of 396 eV and 400 eV to substitutional N (β-N, Ti–N bond) and chemisorbed N_2 (γ-N_2, N–N bond) respectively. Valentin et al. [33,34] assigned the peak with binding energy 400 eV to interstitial N rather than to γ-N_2. This peak has also been correlated to N in NO [40,42]. Chemisorbed N_2 was proposed to assist in visible light absorption but its removal by heat treatment at 350 °C (as seen through XPS) showed no effect to the visible light activity of N doped TiO_2 samples [43].

The ionic radius of N (1.71 Å) is greater than that of O (1.4 Å) which makes its substitution for O site in ZnO and TiO_2 lattice difficult [44]. Reasonably two nitrogen atoms can replace three oxygen atoms to maintain electroneutrality and form an oxygen vacancy [44,45]. The formation energy of oxygen vacancies $(V)_0$ in titania is reduced from 4.2 to 0.6 eV in the presence of nitrogen impurities [33,34]. This indicates that nitrogen doping favors oxygen vacancies formation [33,34]. In anatase N doped TiO_2 the single electron trapped oxygen vacancies were proposed to form a photoactive center with Ti and chemisorbed NO (V_0–NO–Ti) that was visible light sensitive [42]. As mentioned earlier, the oxygen vacancies introduce an absorption band in the visible region from about 400 to 600 nm and make TiO_2 visible light active [26,27]. An absorption or photoluminescence band in the same wavelength range is also observed for N doped samples [33,35,38–44,46]. Consensus is yet to be achieved on if it is the nitrogen atoms substituting oxygen atoms in titania lattice or oxygen vacancies created by nitrogen doping which are responsible for the observed visible light activity of the nitrogen doped samples. Li et al. [45] attributed the visible light activity of the N–TiO_2 samples to the surface porosity, surface texture and doped nitrogen atoms rather than to the oxygen vacancies created by N doping. Ihara et al. [27] prepared visible light responsive TiO_2 polycrystalline samples by a wet chemical method. They considered oxygen vacancies formed in the grain boundaries of the samples to be mainly responsible for the observed visible light activity. The trace amount of the nitrogen that replaced these oxygen deficient sites helped stabilize oxygen vacancies against reoxidation [27]. Zhao et al. considered the oxygen vacancy states generated by nitrogen doping in titania about 1 eV below the CBM as active traps which promoted degradation of methylene blue and methyl orange under visible light irradiation [47]. With an increase in N doping level, the content of oxygen vacancies also increase. These oxygen vacancies can also serve as recombination centers for photogenerated carriers if the N doping level exceeds an optimum level. Experimentally this was observed as a decrease in the quantum yield of $TiO_{2-x}N_x$ samples with increasing x under both UV and visible light irradiation [39].

Various techniques have been employed to dope nitrogen into ZnO and TiO_2 lattice. N substituted ZnO powders have been synthesized by spray pyrolysis [29,30] and dc thermal plasma treatment [31]. Doping of nitrogen in TiO_2 has been mostly carried out under gaseous flow of molecular nitrogen (N_2) [32,36,45], nitrous oxide (N_2O) [44] and ammonia (NH_3) [32,36,39,42,48]. When organic compounds like ammonium carbonate and urea are used as nitrogen sources for doping in titania, they decompose to release ammonia [49]. This ammonia gets adsorbed on the surface of titania and leads to N doping. Amongst various nitrogen doped TiO_2 samples, maximum visible light was absorbed by samples prepared from urea due to higher N concentration [45]. The formation of N_s is favored in Ti rich environment (oxygen deficient environment) like in the presence of NH_3 or N_2 gases whereas N_I or $(NO)_s$ are found to be more stable in O-rich conditions [32–34]. In the intermediate reaction conditions $(NO)_I$ or $(NO_2)_s$ can also become stable in titania lattice [32]. Anatase to rutile transformation was accelerated in the presence of N_2O as a nitrogen source [44]. When N_2 gas was used

to dope N into TiO_2, higher visible light efficiency was achieved at low pressures of N_2 [50] and in the presence of ammonia [51]. The decomposition of molecular nitrogen into atomic N was accelerated by both ammonia and low pressure of N_2. Atomic nitrogen N can be more easily incorporated in titania lattice leading to higher N content in the titania samples [50,51].

Post-sintering has been suggested to improve the visible light efficiency of N–TiO_2 samples prepared by annealing titania in ammonia flow [48]. Post-sintering removed the adsorbed ammonia (that blocks surface active sites), reduced surface oxygen vacancies and favored adsorption of molecular oxygen. However, oxidized nitrogen species formed during the degradation of ethylene covered the surface active sites and reduced the visible light activity of the thermally treated samples [48]. Recently, Yamada et al. [52] studied the effect of post-heat treatment in nitrogen atmosphere and air on N doped TiO_2 samples. In both cases, the visible light activity of the samples decreased owing to the removal of doped nitrogen and creation of oxygen vacancies. In air atmosphere, reoxidation of these vacancies transformed the system to original titania which is inactive under visible light. The photocatalytic efficiency of N doped TiO_2 nanoparticulate films was recovered by removal of gaseous species adsorbed on their surface after MB degradation through a mild heat treatment at 80 °C under nitrogen or argon flow [50].

Ammonia gas usually decomposes to N_2 and H_2 gas at about 550 °C [39]. Therefore ammonia gas serves as both a nitrogen source and as a reducing gas (H_2 gas). Annealing TiO_2 in NH_3 gas flow at high temperatures has many disadvantages. Firstly, the ammonia can be adsorbed on the surface of titania and decrease the surface active sites [48]. Secondly, the surface oxygen defects introduce intragap states which act as recombination centers for photogenerated carriers and lower visible light activity [39]. Since ammonia is a very toxic gas its use as a nitrogen source for doping has been discouraged. Many alternative techniques have been introduced which helps avoid the use of ammonia gas [53–55]. The visible light activity of the nitrogen doped TiO_2 samples prepared by facile hydrothermal method [35] and a simple method using hydrazine as nitrogen source [55] was much higher than that of samples prepared by nitradation of titania in ammonia flow at high temperatures (Table 1).

High hydrogen production has been achieved from titanium dioxide due to cumulative effect of eosin-Y sensitization, N doping and Pt loading [56]. We conjecture that complete mineralization of toxic and hazardous pollutants under visible light irradiation may be achieved by modifying the surface of titania nanoparticles via organic materials or semiconductor coupling in addition to N doping.

4.2. Halogen doping

TiO_2 becomes visible light active when doped with halogens like fluorine [2,57–60] and chlorine [61]. Fluorine atoms easily substitute for O atoms because of their similar ionic radii (1.4 Å for O^{2-} and 1.33 Å for F^-). Chlorine occupies substitutional as well as interstitial sites in TiO_2 lattice with a charge state of −1 [61]. In fluorine doped titania, fluoride ions have been detected not only at substitutional sites in the lattice but also physically adsorbed on the surface of doped TiO_2 nanoparticles [57,58].

No shift in the band edge of titania has been observed with fluorine doping [2] since the F 2p states with high density were calculated to appear below the VB maxima [59]. Although fluorine doping does not modify the electronic structure of TiO_2, visible light activity has been observed with F doped TiO_2 samples [2,60]. Yamaki et al. [59] suggested that visible light absorption might become possible due to the modification of density of states near the CB edge of rutile TiO_2 with fluorine doping [59]. Fluorine doping generates oxygen vacancies and Ti^{3+} states close to the CBM of TiO_2 which are mainly responsible for the observed visible light activity of the doped samples [2,60]. Fluorine converts some Ti^{4+} to Ti^{3+} by charge compensation [57]. These Ti^{3+} donor surface states lie below the CB minima like oxygen vacancies states and help trap photogenerated electrons and molecular oxygen to form superoxide radicals [57]. In contrast to fluorine, chlorine doping introduces new levels in the band gap of titania and enables titania to absorb light with wavelengths as high as 700 nm. The photogenerated electrons can make multiple transitions to the CB of titania via intermediate levels [61].

Chlorine doping lowered the transition temperatures from amorphous to anatase and from anatase to rutile of TiO_2 [61]. Fluorine doping on the other hand suppressed the formation of brookite phase and transformation from anatase to rutile [57]. Contrary to this, fluorine has also been reported to favor formation of rutile phase in TiO_2 [58].

4.3. Sulfur doping

Sulfur can be doped as an anion in titanium dioxide by substituting O sites [62,63] and also as a cation by replacing Ti^{4+} ions in bulk [64] or at the surface [63,65,66]. Substitutional sulfur doping for oxygen sites distorts the crystal lattice due to its large ionic radius (1.8 Å for S^{2-}) compared to that of oxygen (1.4 Å for O^{2-}). Density of states calculations showed that substitutional doping of S in TiO_2 introduces an S 3p band above the valence band edge which can reduce the effective band gap of titania similar to substitutional N doping [36,62].

Co-doping of sulfur as an anion (S^{2-}) and as a cation (S^{4+} and S^{6+}) in TiO_2 helped achieve 85% degradation efficiency of 1-naphthol-5-sulfonic acid (L-acid) under solar light irradiation [63]. High visible light degradation of MB was achieved by Zhou et al. [65] when added sulfur existed as S^{4+} and S^{6+} and as oxidized sulfur species SO_2 and SO_3 adsorbed on the surface of titania. However S doping significantly reduced UV light absorption. Contrary to this, an increase in both UV and visible light absorption and also in UV and visible light activity was noted when sulfur resided as a cation at the surface (S^{6+} in adsorbed SO_4^{2-}) [66]. The adsorbed SO_4^{2-} improved photocatalytic activity by increasing surface acidity and acting as an electron acceptor [66].

4.4. Boron doping

Boron doping in TiO_2 shifts its band edge to higher wavelengths and enhances its visible light absorption [67,68]. B doping in titania is reported to extend its visible light absorption to wavelength as high as 800 nm [67]. XPS studies revealed that B substituted for O sites in titania lattice (active B) [67,68] and also existed as inac-

Table 1
Comparison of the visible light efficiency of N doped TiO_2 samples prepared by various methods to that prepared by annealing in ammonia flow.

Photocatalyst	Synthesis route	Substrate	Visible light efficiency (degradation rates %)	Reference
N–TiO_2	Facile hydrothermal method	Methyl orange	15% degradation in 1 h	[35]
N–TiO_2–NH_3	TiO_2 annealed in NH_3 flow		6% degradation in 1 h	
N–TiO_2	Wet chemical method using hydrazine as N source	Ethylene	9% conversion to CO_2 in 6 h	[55]
N–TiO_2–NH_3	TiO_2 annealed in NH_3 flow		2% conversion to CO_2 in 6 h	

tive oxides of boron (B_2O_3). It is referred to as an inactive oxide under visible light irradiation since it has a wide band gap of 6.3 eV. The B doped TiO_2 sample with highest active B content showed the highest degradation efficiency of methyl tertiary butyl ether (MTBE) under visible light [67]. Zhang and Liu [68] proposed that B doping reduced the band gap of titania by modifying the electronic structure around the conduction band edge.

4.5. Carbon doping

Carbon has been incorporated in titania lattice both as an anion [69] and as a cation [70]. The band gap of titania reduces by carbon doping [69–72]. With incorporation of carbon into titania matrix the conduction band edge shifted to reduce the band gap and surface states were introduced near the valence band edge [72]. The electrons excited from these surface states had the potential to form $O_2^{\bullet-}$ and $^{\bullet}OH$ radicals that efficiently mineralized 4-chlorophenol under visible light irradiation [72]. Carbon doping may form carbonaceous species at the surface of TiO_2 which are reported to facilitate in visible light absorption [69,71]. However they can lower the photocatalytic activity of C doped TiO_2 samples by covering the surface and blocking surface active sites [69].

5. Band gap modification by co-doping of nonmetals

Doping with nonmetals like nitrogen, fluorine, chlorine, sulfur, boron and carbon in TiO_2 has been experimented. These nonmetals make TiO_2 visible light active. The visible light efficiency increases manifold upon co-doping titania with these nonmetals. TiO_2 has been co-doped with N and S [62,66], N and F [45,73,74], and also N and B [67,75]. A marked improvement in the visible light efficiency of the co-doped TiO_2 occurs in comparison to pure and single nonmetal doped titania due to the synergetic effect of the two nonmetals (Table 2).

Compared to pure titania, S–TiO_2 and N–TiO_2 films, N–S co-doped TiO_2 films showed much higher hydrophilicity not only under visible light but also under fluorescent light (UV–vis both) [62]. The simultaneous substitution of N and S for O sites in TiO_2 results in hybridization of N 2p and S 3p bands generated close to the valence band edge which increases hydrophilicity and enhances hole mobility [62]. Visible light degradation of methyl orange was increased by an increase in oxygen vacancies due to N doping and surface acidity by physically adsorbed S in N–S co-doped TiO_2 samples [66]. Simultaneous substitution of N and S narrowed the band gap of TiO_2 and enhanced UV–vis absorption [66].

In N–F co-doped TiO_2, nitrogen doped either substitutionally or as NO_x increased the visible light absorption [45,73,74] while fluorine either substitutionally doped or physically adsorbed at the surface increased the surface acidity, hydroxyl radical formation and active surface sites generation [73]. In et al. [67] found no synergy in the B–N co-doped TiO_2 samples since they showed the same activity under visible light as B-only doped samples. Ling et al. [75] observed synergetic effect of both B and N atoms in co-doped titania. Doping B and N simultaneously narrowed the band gap of titania by modifying electronic structure around the conduction band edge and also increased visible light absorption.

Table 2
Visible light efficiency of co-doped titania samples in comparison to that of pure and single nonmetal doped titania samples.

Photocatalyst	Substrate	Visible light efficiency (degradation rates %)	Reference
TiO_2 (P25)	*p*-Chlorophenol	10% decomposition in 12 h	[73]
F–TiO_2		12% decomposition in 12 h	
N–TiO_2		14% decomposition in 12 h	
N–F co-doped TiO_2		18% decomposition in 12 h	
TiO_2 (P25)	Phenol	15% degradation in 3 h	[75]
B–TiO_2		20% degradation in 3 h	
N–TiO_2		30% degradation in 3 h	
B–F co-doped TiO_2		45% degradation in 3 h	

6. Band gap modification by transition metal doping

ZnO has been doped with various transition metals such as Cu, Co, Mn and Ni [76–86]. When these transition metal ions substitute for Zn^{2+} ions with tetrahedral O coordination in ZnO lattice, the band gap narrows by sp–d exchange interactions between conduction band electrons (CB made up of 4s4p orbitals of Zn) and d electrons of these transition metals [76–80]. Three distinct absorption peaks at 564, 610, and 652 nm appear in the visible region of absorption spectrum of ZnO in case of Co doping corresponding to d–d transitions due to crystal field splitting of 3d levels of Co in ZnO lattice [76–79]. Although Mn doping is mostly reported to introduce defect states close to the conduction band, it may however narrow the band gap by introducing tail states close to the valence band of ZnO [81]. High Mn doping level may also increase the band gap of ZnO [82] due to the Burstein–Moss effect [83]. High visible light activity has been observed with Co and Cu doped ZnO [84–86]. With an increase in Co content in ZnO the absorption of visible light and content of surface oxygen vacancies increased [84]. Visible light decolorization of MB with Co doped ZnO was highest with sample having maximum surface oxygen defects [84]. Co doped ZnO showed better visible light activity than Mn and Ni doped ZnO photocatalysts owing to comparatively better crystallinity and narrower band gap [85].

Ion-implantation technique outclasses chemical sol–gel technique for doping transition metals ions into titania lattice [87,88]. Ion-implantation technique produces more pronounced shift in the band edge of titanium dioxide to visible region [87,88]. Fe doped in TiO_2 through sol–gel technique showed much lower UV and visible photocatalytic activity than with pure titania and Fe ion-implanted titania respectively [88]. Other than Fe, various transition metals like V, Cr, Mn, Co, Ni and Cu have been doped into the bulk of TiO_2 substituting Ti^{4+} ions in the lattice through the ion-implantation method [89]. This results in the overlap of the conduction band due to Ti (3d) with d levels of the transition metals causing red shift of the band edge of TiO_2 [87,89]. Most significant red shift in the absorption edge and an improved visible light activity was manifested by V and Fe ions-implanted TiO_2 [89]. With an increase in ion implantation the visible light efficiency increased but excess metal implantation covered the surface of the titania and lowered the activity [88,89].

Fe doping in titanium dioxide through chemical routes generate impurity states within its band gap [90–92]. Just as by ion implantation, the band gap of titania red shifts by substitution of Fe^{3+} for Ti^{4+} sites through chemical synthesis routes [90–93]. With an increase in Fe content in TiO_2 visible light absorption increased but higher visible light efficiency was achieved at lower concentrations of Fe in TiO_2 [90,91,93]. This is because Fe^{3+} ions actively trap and transfer both photogenerated electrons and holes to the surface of titania at lower level of doping [90,91,93]. At higher concentration these ions serve as recombination centers leading to lower visible light activity [90,91,93]. V doping in TiO_2 films by dip coating technique not only showed high photocatalytic activity but also superhydrophilicity under day light and visible light irradiation simultaneously [94]. Both of these observed effects were explained in terms of band gap narrowing caused by doping. Under visible light irradiation, mesoporous Cr and mesoporous V doped TiO_2 showed much better activity than pure titania and simple Cr or V doped titania [95,96].

Mesoporous Cr–TiO_2 however exhibited much lower UV activity in comparison to pure titania due to increase in surface defects which promoted electron–hole recombination [96].

Pt has been photodeposited as a metallic particle on the surface of titania to scavenge photogenerated electrons due to its suitable Fermi level position [87,97,98]. Pt doping in titania as an ion has been reported to induce visible light activation [99]. Pt doping introduces intragap impurity states which assist valence band electrons to absorb visible light. These states did not serve as recombination centers as indicated by an improvement in both UV and visible light activity of Pt doped titania [99]. Although under visible light irradiation, Pt doped TiO_2 nanoparticles degraded dichloroacetate and 4-CP, they were unable to degrade tetramethylammonium (TMA) and trichloroethylene [99]. Only energetic hydroxyl radicals generated by UV light have the potential to degrade such substrates as TMA.

Transition metals such as Zn, Ag and lanthanides with ionic radii much greater than that of Ti^{4+} cannot be incorporated at Ti sites in TiO_2 lattice [100–102]. Doped Zn was found to be dispersed in the form of ZnO clusters on the surface of the TiO_2 nanocrystallites forming a coupled semiconductor system [100]. The content of surface oxygen vacancies in TiO_2 increased with an increase in the Zn doping concentration. The series of states generated close to the CB of titania and the interfacial coupling between ZnO and TiO_2 particles both narrowed the band gap of TiO_2 making visible light absorption possible [100]. Silver (Ag) gets homogeneously distributed within the titania matrix as metallic silver particles when doped [101]. Ag doping does not modify the band gap of titania but enabled degradation of rhodamine 6G under visible light irradiation due to dye sensitization, absorption of surface plasmon band of Ag around 400 nm and quick scavenging of photogenerated electrons by Ag which retards carrier recombination [101]. Lanthanide ions such as Tb, Eu and Sm were doped on the surface of mesoporous titania nanoparticles [102]. These ions not only prohibited the transformation from anatase to rutile phase but also prevented particles from severely agglomerating [102]. Above an optimum level of Zn and lanthanides doping in TiO_2, the surface oxygen vacancies [100,102] and Ti^{3+} [102] served as recombination centers and lowered the visible light activity of doped samples.

In summary, doping (metals/nonmetals) generates impurity levels in the band gap of semiconductors. If these states lie close to the band edges they can overlap with band states and can narrow the band gap. However, if they are present deep in the band gap they may act as recombination centers for the photogenerated carriers. High photocatalytic activity is achieved if the carriers can be transferred efficiently from these states to the surface. Photocatalytic activity is determined by the competition between this charge carrier promotion rate to surface and the recombination rate. Photogenerated carriers do not get enough time to engage in redox reactions at the surface if the recombination rate is too high. The density of impurity states increase with an increase in the doping level. This can also accelerate recombination process. Doping with both metals and nonmetals makes TiO_2 and ZnO sensitive to visible light. A comparative study show that visible light photocatalytic activity of transition metal ion doped titania is much lower than that of pure titania under solar light (UV–vis both) irradiation [92]. Transition metal doping may lead to loss of crystallinity and phase transformation to rutile, both of which reduce the photocatalytic efficiency [92]. Under solar light irradiation, pure TiO_2 is therefore a better photocatalyst than the metal ion doped TiO_2.

7. Spatially structured and chemically modified visible light active titania

Spatial structuring is a novel physical approach of controlling the size of semiconductor particles from subnanometric to submillimetric length scale [103]. Spatially structured titania photocatalyst in submillimetric length scale can serve as "photonic crystals" [103]. Photonic crystals trap visible photons by increasing the effective light path inside the material which in turn increases the probability of electron excitation owing to longer light/photocatalyst contact time [103]. Highly dispersed and permanently immobilized subnanometric TiO_2 clusters have been formed inside the framework of such microporous hosts as zeolite-Y [103]. The physical approach of spatial structuring of TiO_2 clusters has been respectively integrated with chemical strategies of dye sensitization [104,105], surface-complex assisted sensitization [106] and nitrogen doping [106] to form a bicomponent visible light sensitive and active material. The photoexcited dye ruthenium (II)–tris-bipyridine $[Ru(bpy)_3]^{2+*}$ efficiently injects electrons into the conduction band of nearby titania when both of them are incorporated in the supercages of zeolite-Y [104,105]. The organic modifiers such as benzoic acid, 4-aminobenzoic acid and catechol gets adsorbed on the titania cluster encapsulated in zeolite-Y [106]. The titanol group (Ti^{4+}-OH) of these clusters undergo a condensation reaction with adsorbed organic modifies to form a visible light sensitive complex [106]. However, the adsorbed modifiers reduce the volume of zeolite micropores and slow down the diffusion of substrate (phenol) to active titania surface. Self-degradation of these organic modifiers with the reaction course also lowers the activity of these bicomponent systems. In this respect, nitrogen doped titania clusters encapsulated in zeolite-Y is a stable visible light photocatalyst.

8. Conclusion

TiO_2 has been the focus of major research efforts in the field of photocatalysis due to its high stability. Titania has been made to absorb visible light by spatially structuring it in submillimetric length scale. New techniques of surface-complex assisted sensitization and co-doping of nonmetals have been applied to titania to make it visible light active for the degradation of toxic and hazardous pollutants. Both titania and ZnO have been made active under visible light irradiation by conjugated polymer sensitization. Band gaps of both ZnO and TiO_2 have been modified by nonmetals and transition metals doping. Each dopant has a unique effect on the optical properties and photocatalytic activity of these semiconductor oxides.

Amongst the various techniques employed to make TiO_2 sensitive to visible light co-doping of nonmetals has produced the most appealing results. The synergetic effect of the two nonmetal ions simultaneously doped in TiO_2 produces a remarkable increase in the visible light efficiency of the material. Surface-complex assisted sensitization is a much better alternative to dye sensitization and semiconductor coupling technique since frequent desorption of dyes and decrease in the amount of sensitizer semiconductor can drastically lower the visible light activity of titania. However, these surface complexes can undergo self-degradation with the course of photocatalytic reaction. Although oxygen vacancies can activate TiO_2 under visible light they can also promote electron–hole recombination process.

Boron doping modifies the density of states around the conduction band edge. Further research is required to clarify the nature of the states generated near the conduction band minima. Carbon doping in titania has been less investigated. Detailed study is required to explain various types of carbon species that can be formed on C doping and their effect on the electronic properties of titania. Surface-complex assisted sensitization that has been applied mainly to titania might also activate ZnO under visible light irradiation. Doping with transition metals can prove equally beneficial to nonmetals doping if the amount of dopants and the reaction conditions are properly optimized. The advancements made to date are encouraging and further widens its scope of applicabil-

ity in environmental protection. This paper invites more research for achieving 100% pollutants degradation efficiency with titanium dioxide and zinc oxide semiconductors under both UV and visible light irradiation.

Acknowledgement

Authors are thankful to NUST-School of Electrical Engineering and Computer Science (SEECS) for the provision of facilities to execute the project.

References

[1] T. Bak, J. Nowotny, M. Rekas, C.C. Sorrell, Photo-electrochemical hydrogen generation from water using solar energy. Materials-related aspects, Int. J. Hydrogen Energy 27 (2002) 991–1022.
[2] D. Li, H. Haneda, N.K. Labhsetwar, S. Hishita, N. Ohashi, Visible-light-driven photocatalysis on fluorine-doped TiO_2 powders by the creation of surface oxygen vacancies, Chem. Phys. Lett. 401 (2005) 579–584.
[3] M. Miyauchi, A. Nakajima, T. Watanabe, K. Hashimoto, Photocatalysis and photoinduced hydrophilicity of various metal oxide thin films, Chem. Mater. 14 (2002) 2812–2816.
[4] A. Fujishima, T.N. Rao, D.A. Tryk, Titanium dioxide photocatalysis, J. Photochem. Photobiol. C: Photochem. Rev. 1 (2000) 1–21.
[5] V. Srikant, D.R. Clarkea, On the optical band gap of zinc oxide, J. Appl. Phys. 83 (1998) 5447–5451.
[6] S. Sakthivel, B. Neppolian, M.V. Shankar, B. Arabindoo, M. Palanichamy, V. Murugesan, Solar photocatalytic degradation of azo dye: comparison of photocatalytic efficiency of ZnO and TiO_2, Sol. Energy Mater. Sol. Cells 77 (2003) 65–82.
[7] O.A. Fouad, A.A. Ismail, Z.I. Zaki, R.M. Mohamed, Zinc oxide thin films prepared by thermal evaporation deposition and its photocatalytic activity, Appl. Catal. B: Environ. 62 (2006) 144–149.
[8] A.A. Khodja, T. Sehili, J.-F. Pilichowski, P. Boule, Photocatalytic degradation of 2-phenylphenol on TiO_2 and ZnO in aqueous suspensions, J. Photochem. Photobiol. A: Chem. 141 (2001) 231–239.
[9] D. Chatterjee, S. Dasgupta, Visible light induced photocatalytic degradation of organic pollutants, J. Photochem. Photobiol. C: Photochem. Rev. 6 (2005) 186–205.
[10] D. Chatterjee, A. Mahata, Photosensitized detoxification of organic pollutants on the surface modified TiO_2 semiconductor particulate system, Catal. Commun. 2 (2001) 1–3.
[11] D. Chatterjee, A. Mahata, Visible light induced photodegradation of organic pollutants on dye adsorbed TiO_2 surface, J. Photochem. Photobiol. A: Chem. 153 (2002) 199–204.
[12] J. Moon, C.Y. Yun, K.-W. Chung, M.-S. Kang, J. Yi, Photocatalytic activation of TiO_2 under visible light using Acid Red 44, Catal. Today 87 (2003) 77–86.
[13] S. Kaur, V. Singh, Visible light induced sonophotocatalytic degradation of Reactive Red dye 198 using dye sensitized TiO_2, Ultrason. Sonochem. 14 (2007) 531–537.
[14] R. Abe, K. Hara, K. Sayamaa, K. Domen, H. Arakawa, Steady hydrogen evolution from water on eosin Y-fixed TiO_2 photocatalyst using a silane-coupling reagent under visible light irradiation, J. Photochem. Photobiol. A: Chem. 137 (2000) 63–69.
[15] J. Zhao, C. Chen, W. Ma, Photocatalytic degradation of organic pollutants under visible light irradiation, Top. Catal. 35 (2005) 269–278.
[16] D. Jiang, Y. Xu, B. Hou, D. Wu, Y. Sun, Synthesis of visible light-activated TiO_2 photocatalyst via surface organic modification, J. Solid State Chem. 180 (2007) 1787–1791.
[17] M. Li, P. Tang, Z. Hong, M. Wang, High efficient surface-complex-assisted photodegradation of phenolic compounds in single anatase titania under visible-light, Colloids Surf. A: Physicochem. Eng. Aspects 318 (2008) 285–290.
[18] D. Jiang, Y. Xu, D. Wu, Y. Sun, Visible-light responsive dye-modified TiO_2 photocatalyst, J. Solid State Chem. 181 (2008) 593–602.
[19] L. Song, R. Qiu, Y. Mo, D. Zhang, H. Wei, Y. Xiong, Photodegradation of phenol in a polymer-modified TiO_2 semiconductor particulate system under the irradiation of visible light, Catal. Commun. 8 (2007) 429–433.
[20] R. Qiu, D. Zhang, Y. Mo, L. Song, E. Brewer, X. Huang, Y. Xiong, Photocatalytic activity of polymer-modified ZnO under visible light irradiation, J. Hazard. Mater. 156 (2008) 80–85.
[21] Y. Bessekhouad, D. Robert, J.V. Weber, Bi_2S_3/TiO_2 and CdS/TiO_2 heterojunctions as an available configuration for photocatalytic degradation of organic pollutant, J. Photochem. Photobiol. A: Chem. 163 (2004) 569–580.
[22] L. Wu, J.C. Yu, X. Fua, Characterization and photocatalytic mechanism of nanosized CdS coupled TiO_2 nanocrystals under visible light irradiation, J. Mol. Catal. A: Chem. 244 (2006) 25–32.
[23] S.M. Ji, H. Jun, J.S. Jang, H.C. Son, P.H. Borse, J.S. Lee, Photocatalytic hydrogen production from natural seawater, J. Photochem. Photobiol. A: Chem. 189 (2007) 141–144.
[24] W. Ho, J.C. Yu, Sonochemical synthesis and visible light photocatalytic behavior of CdSe and $CdSe/TiO_2$ nanoparticles, J. Mol. Catal. A: Chem. 247 (2006) 268–274.
[25] L. Jianhua, Y. Rong, L. Songmei, Preparation and characterization of the TiO_2–V_2O_5 photocatalyst with visible-light activity, Rare Met. 25 (2006) 636–642.
[26] I. Nakamura, N. Negishi, S. Kutsuna, T. Ihara, S. Sugihara, K. Takeuch, Role of oxygen vacancy in the plasma-treated TiO_2 photocatalyst with visible light activity for NO removal, J. Mol. Catal. A: Chem. 161 (2000) 205–212.
[27] T. Ihara, M. Miyoshi, Y. Iriyama, O. Matsumoto, S. Sugihara, Visible-light-active titanium oxide photocatalyst realized by an oxygen-deficient structure and by nitrogen doping, Appl. Catal. B: Environ. 42 (2003) 403–409.
[28] I. Justicia, G. Garcia, G.A. Battiston, R. Gerbasi, F. Ager, M. Guerra, J. Caixach, J.A. Pardo, J. Riverad, A. Figueras, Photocatalysis in the visible range of substoichiometric anatase films prepared by MOCVD, Electrochim. Acta 50 (2005) 4605–4608.
[29] D. Li, H. Haneda, Synthesis of nitrogen-containing ZnO powders by spray pyrolysis and their visible-light photocatalysis in gas-phase acetaldehyde decomposition, J. Photochem. Photobiol. A: Chem. 155 (2003) 171–178.
[30] D. Li, H. Haneda, Photocatalysis of sprayed nitrogen-containing Fe_2O_3–ZnO and WO_3–ZnO composite powders in gas-phase acetaldehyde decomposition, J. Photochem. Photobiol. A: Chem. 160 (2003) 203–212.
[31] H.F. Lin, S.C. Liao, S.W. Hung, The dc thermal plasma synthesis of ZnO nanoparticles for visible-light photocatalyst, J. Photochem. Photobiol. A: Chem. 174 (2005) 82–87.
[32] R. Asahi, T. Morikawa, Nitrogen complex species and its chemical nature in TiO_2 for visible-light sensitized photocatalysis, Chem. Phys. 339 (2007) 57–63.
[33] C.D. Valentin, G. Pacchioni, A. Selloni, S. Livraghi, E. Giamello, Characterization of paramagnetic species in N-doped TiO_2 powders by EPR spectroscopy and DFT calculations, J. Phys. Chem. B 109 (2005) 11414–11419.
[34] C.D. Valentin, E. Finazzi, G. Pacchioni, A. Selloni, S. Livraghi, M.C. Paganini, E. Giamello, N-doped TiO_2: theory and experiment, Chem. Phys. 339 (2007) 44–56.
[35] F. Peng, L. Cai, L. Huang, H. Yu, H. Wang, Preparation of nitrogen-doped titanium dioxide with visible-light photocatalytic activity using a facile hydrothermal method, J. Phys. Chem. Solids 69 (2008) 1657–1664.
[36] R. Asahi, T. Morikawa, T. Ohwaki, K. Aoki, Y. Taga, Visible-light photocatalysis in nitrogen-doped titanium oxides, Science 293 (2001) 269–271.
[37] H. Shen, L. Mi, P. Xu, W. Shen, P.-N. Wang, Visible-light photocatalysis of nitrogen-doped TiO_2 nanoparticulate films prepared by low-energy ion implantation, Appl. Surf. Sci. 253 (2007) 7024–7028.
[38] F. Peng, L. Cai, H. Yu, H. Wang, J. Yang, Synthesis and characterization of substitutional and interstitial nitrogen-doped titanium dioxides with visible light photocatalytic activity, J. Solid State Chem. 181 (2008) 130–136.
[39] H. Irie, Y. Watanabe, K. Hashimoto, Nitrogen-concentration dependence on photocatalytic activity of $TiO_{2-x}N_x$ powders, J. Phys. Chem. B 107 (2003) 5483–5486.
[40] S. Sato, R. Nakamura, S. Abe, Visible-light sensitization of TiO_2 photocatalysts by wet method N doping, Appl. Catal. A: Gen. 284 (2005) 131–137.
[41] X. Chen, P.-A. Glans, X. Qiu, S. Dayal, W.D. Jennings, K.E. Smith, C. Burda, J. Guo, X-ray spectroscopic study of the electronic structure of visible-light responsive N-, C- and S-doped TiO_2, J. Electron Spectrosc. Relat. Phenom. 162 (2008) 67–73.
[42] J. Zhang, Y. Wang, Z. Jin, Z. Wu, Z. Zhang, Visible-light photocatalytic behavior of two different N-doped TiO_2, Appl. Surf. Sci. 254 (2008) 4462–4466.
[43] J. Yuan, M. Chen, J. Shi, W. Shangguan, Preparations and photocatalytic hydrogen evolution of N doped TiO_2 from urea and titanium tetrachloride, Int. J. Hydrogen Energy 31 (2006) 1326–1331.
[44] Y. Guo, X.-w. Zhang, W.-H. Weng, G.-r. Han, Structure and properties of nitrogen-doped titanium dioxide thin films grown by atmospheric pressure chemical vapor deposition, Thin Solid Films 515 (2007) 7117–7121.
[45] D. Li, H. Haneda, S. Hishita, N. Ohash, Visible-light-driven nitrogen-doped TiO_2 photocatalysts: effect of nitrogen precursors on their photocatalysis for decomposition of gas-phase organic pollutants, Mater. Sci. Eng. B 117 (2005) 67–75.
[46] A.P. Huang, Z.F. Di, P.K. Chu, Microstructure and visible-photoluminescence of titanium dioxide thin films fabricated by dual cathodic arc and nitrogen plasma deposition, Surf. Coat. Technol. 201 (2007) 4897–4900.
[47] L. Zhao, Q. Jiang, J. Lian, Visible-light photocatalytic activity of nitrogen-doped TiO_2 thin film prepared by pulsed laser deposition, Appl. Surf. Sci. 254 (2008) 4620–4625.
[48] X. Chen, X. Wang, Y. Hou, J. Huang, L. Wu, X. Fu, The effect of postnitridation annealing on the surface property and photocatalytic performance of N-doped TiO_2 under visible light irradiation, J. Catal. 255 (2008) 59–67.
[49] S. Yin, K. Ihara, M. Komatsu, Q. Zhang, F. Saito, T. Kyotani, T. Sato, Low temperature synthesis of $TiO_{2-x}N_y$ powders and films with visible light responsive photocatalytic activity, Solid State Commun. 137 (2006) 132–137.
[50] L. Mi, P. Xu, H. Shen, P.-N. Wang, Recovery of visible-light photocatalytic efficiency of N-doped TiO_2 nanoparticulate films, J. Photochem. Photobiol. A: Chem. 193 (2008) 222–227.
[51] S. Somekawa, Y. Kusumoto, M. Ikeda, B. Ahmmad, Y. Horie, Fabrication of N-doped TiO_2 thin films by laser ablation method: mechanism of N-doping and evaluation of the thin films, Catal. Commun. 9 (2008) 437–440.
[52] K. Yamada, H. Yamane, S. Matsushima, H. Nakamura, K. Ohira, M. Kouya, K. Kumada, Effect of thermal treatment on photocatalytic activity of N-doped TiO_2 particles under visible light, Thin Solid Films 516 (2008) 7482–7487.
[53] A.R. Gandhe, J.B. Fernandes, A simple method to synthesize visible light active N-doped anatase (TiO_2) photocatalyst, Bull. Catal. Soc. India 4 (2005) 131–134.

[54] W. Zuyuan, Z. Fuxiang, Y. Yali, C. Jie, S. Qing, G. Naijia, One-pot synthesis of visible-light-responsive TiO_2 in the presence of various amines, Chin. J. Catal. 27 (2006) 1091–1095.
[55] D. Li, H. Huang, X. Chen, Z. Chen, W. Li, D. Ye, X. Fu, New synthesis of excellent visible-light $TiO_{2-x}N_x$ photocatalyst using a very simple method, J. Solid State Chem. 180 (2007) 2630–2634.
[56] Y. Li, C. Xie, S. Peng, G. Lu, S. Li, Eosin Y-sensitized nitrogen-doped TiO_2 for efficient visible light photocatalytic hydrogen evolution, J. Mol. Catal. A: Chem. 282 (2008) 117–123.
[57] J.C. Yu, J. Yu, W. Ho, Z. Jiang, L. Zhang, Effects of F-doping on the photocatalytic activity and microstructures of nanocrystalline TiO_2 powders, Chem. Mater. 14 (2002) 3808–3816.
[58] N. Todorova, T. Giannakopoulou, G. Romanos, T. Vaimakis, J. Yu, C. Trapalis, Preparation of fluorine-doped TiO_2 photocatalysts with controlled crystalline structure, Int. J. Photoenergy (2008) (Article ID 534038, pp. 1–9).
[59] T. Yamaki, T. Umebayashi, T. Sumita, S. Yamamoto, M. Maekawa, A. Kawasuso, H. Itoh, Fluorine-doping in titanium dioxide by ion implantation technique, Nucl. Instrum. Methods Phys. Res. B 206 (2003) 254–258.
[60] G. Wu, A. Chen, Direct growth of F-doped TiO_2 particulate thin films with high photocatalytic activity for environmental applications, J. Photochem. Photobiol. A: Chem. 195 (2008) 47–53.
[61] L. Mingce, C. Weimin, C. Heng, X. Jun, Preparation, characterization and photocatalytic activity of visible light driven chlorine-doped TiO_2, Front. Chem. China 2 (3) (2007) 278–282.
[62] T. Ohno, M. Akiyoshi, T. Umebayashi, K. Asai, T. Mitsui, M. Matsumura, Preparation of S-doped TiO_2 photocatalysts and their photocatalytic activities under visible light, Appl. Catal. A: Gen. 265 (2004) 115–121.
[63] Y.W. Sakai, K. Obata, K. Hashimoto, H. Irie, Enhancement of visible light-induced hydrophilicity on nitrogen and sulfur-codoped TiO_2 thin films, Vacuum 83 (2009) 683–687.
[64] Y. Wang, J. Li, P. Peng, T. Lu, L. Wang, Preparation of S-TiO_2 photocatalyst and photodegradation of L-acid under visible light, Appl. Surf. Sci. 254 (2008) 5276–5280.
[65] Z. Zhou, J. Wang, S. Zhou, X. Liu, G. Meng, Processing TiO_2 in gaseous sulfur and research on its photocatalysis under visible light, Catal. Commun. 9 (2008) 568–571.
[66] F. Wei, L. Ni, P. Cui, Preparation and characterization of N–S-codoped TiO_2 photocatalyst and its photocatalytic activity, J. Hazard. Mater. 156 (2008) 135–140.
[67] S. In, A. Orlov, R. Berg, F. Garcıa, S. Pedrosa-Jimenez, M.S. Tikhov, D.S. Wright, R.M. Lambert, Effective visible light-activated B-doped and B,N-codoped TiO_2 photocatalysts, J. Am. Chem. Soc. 129 (2007) 13790–13791.
[68] X. Zhang, Q. Liu, Preparation and characterization of titania photocatalyst co-doped with boron, nickel, and cerium, Mater. Lett. 62 (2008) 2589–2592.
[69] C. Xu, R. Killmeyer, M.L. Gray, S.U.M. Khan, Photocatalytic effect of carbon-modified *n*-TiO_2 nanoparticles under visible light illumination, Appl. Catal. B: Environ. 64 (2006) 312–317.
[70] W. Ren, Z. Ai, F. Jia, L. Zhang, X. Fan, Z. Zou, Low temperature preparation and visible light photocatalytic activity of mesoporous carbon-doped crystalline TiO_2, Appl. Catal. B: Environ. 69 (2007) 138–144.
[71] M.-S. Wong, S.-W. Hsu, K.K. Rao, C.P. Kumar, Influence of crystallinity and carbon content on visible light photocatalysis of carbon doped titania thin films, J. Mol. Catal. A: Chem. 279 (2008) 20–26.
[72] S. Sakthivel, H. Kisch, Daylight photocatalysis by carbon-modified titanium dioxide, Angew. Chem. Int. Ed. 42 (2003) 4908–4911.
[73] D.-G. Huang, S.-J. Liao, J.-M. Liu, Z. Dang, L. Petrik, Preparation of visible-light responsive N–F-codoped TiO_2 photocatalyst by a sol–gel-solvothermal method, J. Photochem. Photobiol. A: Chem. 184 (2006) 282–288.
[74] Y. Xie, Y. Li, X. Zhao, Low-temperature preparation and visible-light-induced catalytic activity of anatase F–N-codoped TiO_2, J. Mol. Catal. A: Chem. 277 (2007) 119–126.
[75] Q. Ling, J. Sun, Q. Zhou, Preparation and characterization of visible-light-driven titania photocatalyst co-doped with boron and nitrogen, Appl. Surf. Sci. 254 (2008) 3236–3241.
[76] S. Deka, P.A. Joy, Electronic structure and ferromagnetism of polycrystalline $Zn_{1-x}Co_xO$ ($0 \le x \le 0.15$), Solid State Commun. 134 (2005) 665–669.
[77] C.B. Fitzgerald, M. Venkatesan, J.G. Lunney, L.S. Dorneles, J.M.D. Coey, Cobalt-doped ZnO—a room temperature dilute magnetic semiconductor, Appl. Surf. Sci. 247 (2005) 493–496.
[78] S. Colis, H. Bieber, S. Bégin-Colin, G. Schmerber, C. Leuvrey, A. Dinia, Magnetic properties of Co-doped ZnO diluted magnetic semiconductors prepared by low-temperature mechanosynthesis, Chem. Phys. Lett. 422 (2006) 529–533.
[79] M. Naeem, S.K. Hasanain, A. Mumtaz, Electrical transport and optical studies of ferromagnetic cobalt doped ZnO nanoparticles exhibiting a metal–insulator transition, J. Phys. Condens. Matter 20 (2008) 7.
[80] V.R. Shinde, T.P. Gujar, C.D. Lokhande, R.S. Mane, S.-H. Han, Mn doped and undoped ZnO films: a comparative structural, optical and electrical properties study, Mater. Chem. Phys. 96 (2006) 326–330.
[81] R. Ullah, J. Dutta, Photocatalytic degradation of organic dyes with manganese-doped ZnO nanoparticles, J. Hazard. Mater. 156 (2008) 194–200.
[82] Y.S. Wang, P.J. Thomas, P. O'Brien, Optical properties of ZnO nanocrystals doped with Cd, Mg, Mn, and Fe ions, J. Phys. Chem. B 110 (2006) 21412–21415.
[83] G. Srinivasana, J. Kumar, Effect of Mn doping on the microstructures and optical properties of sol–gel derived ZnO thin films, J. Cryst. Growth 310 (2008) 1841–1846.
[84] Q. Xiao, J. Zhang, C. Xiao, X. Tan, Photocatalytic decolorization of methylene blue over $Zn_{1-x}Co_xO$ under visible light irradiation, Mater. Sci. Eng. B 142 (2007) 121–125.
[85] S. Ekambaram, Y. Iikubo, A. Kudo, Combustion synthesis and photocatalytic properties of transition metal-incorporated ZnO, J. Alloys Compd. 433 (2007) 237–240.
[86] K.G. Kanade, B.B. Kale, J.O. Baeg, S.M. Lee, C.W. Lee, S.J. Moon, H. Chang, Self-assembled aligned Cu doped ZnO nanoparticles for photocatalytic hydrogen production under visible light irradiation, Mater. Chem. Phys. 102 (2007) 98–104.
[87] M. Anpo, M. Takeuchi, The design and development of highly reactive titanium oxide photocatalysts operating under visible light irradiation, J. Catal. 216 (2003) 505–516.
[88] H. Yamashita, M. Harada, J. Misaka, M. Takeuchi, B. Neppolian, M. Anpo, Photocatalytic degradation of organic compounds diluted in water using visible light-responsive metal ion-implanted TiO_2 catalysts: Fe ion-implanted TiO_2, Catal. Today 84 (2003) 191–196.
[89] H. Yamashita, M. Harada, J. Misaka, M. Takeuchi, K. Ikeue, M. Anpo, Degradation of propanol diluted in water under visible light irradiation using metal ion-implanted titanium dioxide photocatalysts, J. Photochem. Photobiol. A: Chem. 148 (2002) 257–261.
[90] W.-C. Hung, S.-H. Fu, J.-J. Tseng, H. Chu, T.-H. Ko, Study on photocatalytic degradation of gaseous dichloromethane using pure and iron ion-doped TiO_2 prepared by the sol–gel method, Chemosphere 66 (2007) 2142–2151.
[91] Mst. S. Nahar, K. Hasegawa, S. Kagaya, Photocatalytic degradation of phenol by visible light-responsive iron-doped TiO_2 and spontaneous sedimentation of the TiO_2 particles, Chemosphere 65 (2006) 1976–1982.
[92] P. Bouras, E. Stathatos, P. Lianos, Pure versus metal-ion-doped nanocrystalline titania for photocatalysis, Appl. Catal. B: Environ. 73 (2007) 51–59.
[93] Z. Ambrus, N. Balázs, T. Alapi, G. Wittmann, P. Sipos, A. Dombi, K. Mogyorósi, Synthesis, structure and photocatalytic properties of Fe(III)-doped TiO_2 prepared from $TiCl_3$, Appl. Catal. B: Environ. 81 (2008) 27–37.
[94] H. Li, G. Zhao, G. Han, B. Song, Hydrophilicity and photocatalysis of $Ti_{1-x}V_xO_2$ films prepared by sol–gel method, Surf. Coat. Technol. 201 (2007) 7615–7618.
[95] D. Masih, H. Yoshitake, Y. Izumi, Photo-oxidation of ethanol on mesoporous vanadium–titanium oxide catalysts and the relation to vanadium (IV) and (V) sites, Appl. Catal. A: Gen. 325 (2007) 276–282.
[96] X. Fan, X. Chen, S. Zhu, Z. Li, T. Yu, J. Ye, Z. Zou, The structural, physical and photocatalytic properties of the mesoporous Cr-doped TiO_2, J. Mol. Catal. A: Chem. 284 (2008) 155–160.
[97] D. Hufschmidt, D. Bahnemanna, J.J. Testa, C.A. Emilio, M.I. Litter, Enhancement of the photocatalytic activity of various TiO_2 materials by platinisation, J. Photochem. Photobiol. A: Chem. 148 (2002) 223–231.
[98] T.A. Egerton, J.A. Mattinson, The influence of platinum on UV and 'visible' photocatalysis by rutile and Degussa P25, J. Photochem. Photobiol. A: Chem. 194 (2008) 283–289.
[99] S. Kim, S.-J. Hwang, W. Choi, Visible light active platinum-ion-doped TiO_2 photocatalyst, J. Phys. Chem. B 109 (2005) 24260–24267.
[100] Y. Zhao, C. Li, X. Liu, F. Gu, H.L. Du, L. Shi, Zn-doped TiO_2 nanoparticles with high photocatalytic activity synthesized by hydrogen–oxygen diffusion flame, Appl. Catal. B: Environ. 79 (2008) 208–215.
[101] M.K. Seery, R. George, P. Floris, S.C. Pillai, Silver doped titanium dioxide nanomaterials for enhanced visible light photocatalysis, J. Photochem. Photobiol. A: Chem. 189 (2007) 258–263.
[102] M. Saif, M.S.A. Abdel-Mottaleb, Titanium dioxide nanomaterial doped with trivalent lanthanide ions of Tb, Eu and Sm: preparation, characterization and potential applications, Inorg. Chim. Acta 360 (2007) 2863–2874.
[103] C. Aprile, A. Corma, H. Garcia, Enhancement of the photocatalytic activity of TiO_2 through spatial structuring and particle size control: from subnanometric to submillimetric length scale, Phys. Chem. Chem. Phys. 10 (2008) 769–783.
[104] S.H. Bossmann, S. Jockusch, P. Schwarz, B. Baumeister, S. Göb, C. Schnabel, L. Payawan Jr., M.R. Pokhrel, M. Wörner, A.M. Braun, N.J. Turro, Ruthenium(II)–tris-bipyridine/titanium dioxide codoped zeolite Y photocatalysts. II. Photocatalyzed degradation of the model pollutant 2,4-xylidine, evidence for percolation behavior, Photochem. Photobiol. Sci. 2 (2003) 477–486.
[105] S.H. Bossmann, C. Turro, C. Schnabel, M.R. Pokhrel, L.M. Payawan Jr., B. Baumeister, M. Wörner, $Ru(bpy)_3^{2+}$/TiO_2-codoped zeolites: synthesis, characterization, and the role of TiO_2 in electron transfer photocatalysis, J. Phys. Chem. B 105 (2001) 5374–5382.
[106] M. Alvaro, E. Carbonell, V. Fornés, H. Garcia, Enhanced photocatalytic activity of zeolite-encapsulated TiO_2 clusters by complexation with organic additives and N-doping, ChemPhysChem 7 (2006) 200–205.